On inversion-based approaches for feedforward and ILC☆

Jurgen van Zundert[a,*], Tom Oomen[a]

[a] *Control Systems Technology, Department of Mechanical Engineering, Eindhoven University of Technology, Eindhoven, The Netherlands*

Abstract

System inversion is at the basis of many feedforward and learning control algorithms. The aim of this paper is to analyze several of these approaches in view of their subsequent use, showing inappropriate use that is previously overlooked. This leads to different insights and new approaches for both feedforward and learning. The methods are compared in various aspects, including finite vs. infinite preview, exact vs. approximate, and quality of inversion in various norms which directly relates to their use. In addition, extensions to (non-square) multivariable and time-varying systems are presented. The results are validated on a nonminimum-phase benchmark system.

Keywords: Model inversion, Nonminimum phase, Feedforward control, ILC

1. Introduction

The quality of inversion depends on the goal one has in mind. The aim of this paper is to investigate, compare, and develop inversion techniques for the purpose of both feedforward and learning control. The model to be inverted includes the closed-loop process sensitivity in iterative learning control (ILC) [1, 2], the closed-loop complementary sensitivity in repetitive control [3], or the open-loop system in inverse model feedforward [4]. For nonminimum-phase or strictly proper systems, such inversion is not always straightforward. In addition, multivariable systems and time varying systems impose additional complications.

System inversion has received significant attention, also from a theoretical perspective [5]. Successful approximate solutions include [6], ZPETC [7], ZMETC, NPZ-Ignore [8], and EBZPETC [9], see also [10] for an overview. Additionally, standard $\mathcal{H}_\infty$ without preview has been used [11, 12] to design ILC filters, as well as $\mathcal{H}_\infty$ preview in feedforward [13, 14]. Furthermore, optimization-based approaches include techniques based on LQ tracking control [15], also known as norm-optimal ILC [16], where in addition to inversion a weight on the input signal is imposed. In [17], ZPETC, ZMETC, and a model matching approach are compared. The model matching approach is similar to the $\mathcal{H}_\infty$ preview control presented in the present work, yet without preview.

Although many algorithms and approaches are available for model inversion, the choice for a technique is sometimes made arbitrarily without a full understanding of the alternatives and their underlying mechanisms. For example, ZPETC is often used for the design of ILC filters, but requires an additional robustness filter at the cost of performance [2, 18]. Alternatively, infinite preview [19] or $\mathcal{H}_\infty$ based [11, 12] techniques can be used. However, [11, 12] lack the use of preview, and are recently extended in [20] towards preview/fixed lag smoothing situations.

This paper provides guidelines on proper use of inversion techniques for both inverse model feedforward and learning control by addressing the application specific objective. The aim of this paper is to compare existing approaches and provide several new approaches with clear benefits. In this regard, it extends [10, 21] with additional approaches, by explicitly addressing the control goal, and investigating applicability to non-square multivariable and time varying systems. It also extends [19] in which technical results on several algorithms are presented by evaluating them in a broader perspective.

The outline of the paper is as follows. In section 2, the inverse model feedforward and ILC optimization problems are cast in a single general framework, and the associated challenges, optimization criteria, and properties are presented. In section 3, the benchmark system used for assessing the inversion techniques is introduced. In section 4, the inversion techniques are presented. First, the well-known approximate inverse techniques NPZ-Ignore, ZPETC, and ZMETC, and the stable inversion technique are recapitulated. Second, inversion techniques based on norm-optimal feedforward/ILC is presented. Third, $\mathcal{H}_\infty$ and $\mathcal{H}_2$ preview control are presented. In section 5, the techniques are evaluated on the benchmark system of section 3 in both a feedforward and an ILC setting. In section 6, a two-step approach for inversion of non-square systems is presented. In section 7, the one-step techniques of section 4 are extended to multivariable and time varying

☆This work is part of the research programme Robust Cyber-Physical Systems (RCPS) (No. 12694) and Innovational Research Incentives Scheme under the VENI grant "Precision Motion: Beyond the Nanometer" (No. 13073); both are (partly) financed by the Netherlands Organisation for Scientific Research (NWO).

*Corresponding author. E-mail: j.c.d.v.zundert@tue.nl

Table 1
Conversion from feedforward (Fig. 1(a)) and ILC (Fig. 1(b)) into the general diagram of Fig. 1(c).

	r	F	u	H	W	e
feedforward	r	F	f	G	S	e
ILC	e_j	L	$f_{j+1} - f_j$	SG	1	e_{j+1}

systems. Section 8 contains conclusions and recommendations.

Notation. Apart from section 7, discrete, single-input, single-output (SISO), linear, time invariant (LTI) systems are considered. In section 7, extensions to multi-input, multi-output (MIMO) and linear time varying (LTV) systems are presented. Let $S = (1 + GC)^{-1}$ denote the sensitivity and $\lambda_i(\cdot)$ the ith eigenvalue. A causal LTI system is referred to as stable (minimum phase) iff all poles (zeros) are inside the unit circle, otherwise the system is referred to as unstable (nonminimum phase). For ease of presentation, it is assumed that the inverted system is hyperbolic, i.e., contains no eigenvalues on the unit circle. Note that techniques as in [22] can be used to relax this condition.

2. Problem definition

In this section, the inverse model feedforward and ILC optimization problem are detailed, the common inversion problem is formulated, and the application specific criteria are defined.

2.1. Role of inversion for feedforward and ILC

Feedback and feedforward control are typically combined to achieve high performance. Feedback control can deal with uncertainty, but its performance is limited due to Bode's sensitivity integral. For known signals, feedforward control can be used to achieve excellent performance. In the feedforward scheme of Fig. 1(a), the goal is to design feedforward f such that tracking error $e = r - y$ is minimized, where r is the desired trajectory for output y. If the system performs repetitive trajectories r, information of the previous task j can be used to enhance the performance of the next task $j+1$ through iterative learning control (ILC). For the ILC scheme of Fig. 1(b), f_{j+1} is designed based on data e_j, f_j such that $e_{j+1} = e_j - SG(f_{j+1} - f_j)$ is minimized.

Both the feedforward and the ILC design problem can be cast into the diagram of Fig. 1(c). As shown by Table 1, both problems are equivalent to finding an input u such that error e is minimized. System H can be an open-loop system as in feedforward (G) or a closed-loop system as in ILC (SG) and repetitive control (RC) (SGC).

2.2. On inversion

Consider the general block diagram in Fig. 1(c). Throughout, it is assumed that system H is proper with relative degree $d \in \mathbb{N}$, has $p \in \mathbb{N}$ nonminimum-phase zeros,

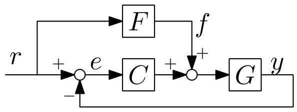

(a) Feedforward control.

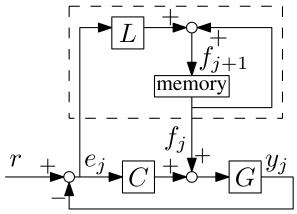

(b) Iterative learning control.

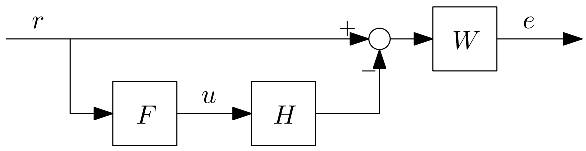

(c) General block diagram.

Fig. 1. The feedforward (a) and ILC (b) design problem are equivalent to finding u in (c) that minimizes e.

and has state-space realization (A, B, C, D). An immediate solution to minimize e is to select $F = H^{-1}$, where

$$H^{-1} \overset{s}{=} \left[\begin{array}{c|c} A - BD^{-1}C & BD^{-1} \\ \hline -D^{-1}C & D^{-1} \end{array}\right]. \tag{1}$$

At least three challenges are associated with the direct use of (1):

I) Delay: for $d > 0$, H^{-1} does not exist since D is not invertible.

II) Non-square: systems with a different number of inputs then outputs cannot be directly inverted as in (1) since D is non-square.

III) Nonminimum-phase zeros: for $p > 0$, H^{-1} is unstable which, when solved forward in time, yields unbounded u.

This paper mainly focuses on the third challenge.

Remark 1. The first issue can be overcome by inverting the bi-proper system $\bar{H} = z^d H$, where the a-causal z^d is implemented as a time-shift on the time domain signal. Note that for an infinite time horizon, filtering the time-shifted signal with $\bar{H}$ is equivalent to filtering the original signal with H, whereas for a finite time horizon this might introduce boundary errors.

Remark 2. The second issue can be overcome by using the two-step procedure presented in section 6.

2.3. Criteria

Depending on H, it might not be possible to achieve zero error $e = 0$. Therefore, the inversion techniques construct u given a certain criterion aimed at minimizing e. The criterion depends on the particular application.

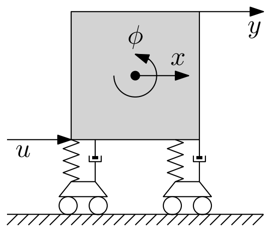

Fig. 2. The benchmark system is a mass that can translate in x direction and rotate in ϕ direction. The system has input force u and output position y.

In feedforward, generally high performance in terms of the error e is pursued. Typically, this is enforced by minimizing the energy in the error signal through minimizing $\|e\|_2$ [23, 4].

In ILC, the main concern is to guarantee convergence in the error to ensure stability over trails. Superior performance is obtained by executing several trials. For update $f_{j+1} = f_j + Le_j$, see also Fig. 1(b), the error has trial dynamics $e_{j+1} = (1 - SGL)\, e_j$. Hence, to ensure the convergence of $\|e_j\|_2$ over trials it should hold $\|1 - SGL\|_\infty < 1$ [3]. Note that this is equivalent to monotonic convergence of $\|e_j - e_\infty\|_2$. Assuming this is feasible, the fastest convergence for arbitrary e_j is found by minimizing $\|1 - SGL\|_\infty$. In the general block diagram of Fig. 1(c), this is equivalent to minimizing $\|W(1 - HF)\|_\infty$. Optionally, if convergence cannot be guaranteed, a robustness filter Q can be added as $f_{j+1} = Q(f_j + Le_j)$ with corresponding convergence condition $\|Q(1 - SGL)\|_\infty < 1$. If the model is uncertain, the condition can be evaluated for the uncertain model or for the frequency response function of SG.

2.4. Properties

In section 4, a variety of inversion techniques is presented. The main properties of these techniques are:

- Finite vs. infinite horizon design;
- Finite vs. infinite preview, i.e., the required amount of future input data;
- Applicability to SISO, MIMO, and non-square systems;
- Applicability to time invariant and time varying systems;
- Design objective.

An overview of these properties for the techniques in section 4 is listed in section 5.

3. Benchmark system

To validate the inversion techniques of section 4, the benchmark system shown in Fig. 2 is used. The same system is used in [19] for different purposes.

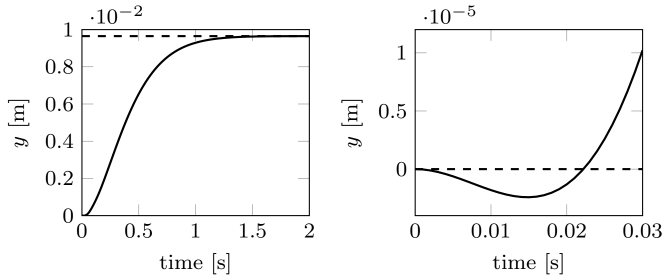

(a) Response to positive step. **(b)** Initially, the system moves in negative direction.

Fig. 3. Step response of SG. The nonminimum-phase character of the system is reflected in the system initially moving in opposite direction.

The open-loop system G from force u [N] to position y [m] in Fig. 2 is given by

$$G(z) = \frac{-3 \times 10^{-8}(z + 0.9632)(z - 0.9447)(z - 1.1410)}{(z - 1)^2(z^2 - 1.9595z + 0.9632)},$$

with sample time $h = 0.001$ s. The closed-loop system SG with feedback controller $C(z) = \frac{925(z-0.9979)}{z-0.9813}$ is given by

$$SG(z) = \frac{-3 \times 10^{-8}(z + 0.9632)(z - 0.9447)}{(z - 0.9901)(z^2 - 1.9903z + 0.9903)} \times \frac{(z - 1.1410)(z - 0.9813)}{(z^2 - 1.9605z + 0.9640)}.$$

For both $H = G$ in feedforward and $H = SG$ in ILC, the following observations can be made:

- H is stable ($|\lambda_i(H)| \leq 1$, $\forall i$);
- H has one nonminimum-phase zero $z = 1.1410$ ($p = 1$);
- H is strictly proper ($D = 0$) with relative degree $d = 1$ (see also Remark 1).

The step response for SG is shown in Fig. 3. Due to the single nonminimum-phase zero, the system initially moves in opposite direction [24].

The reference trajectory r is a fourth-order forward-backward motion of total length $N = 4201$ samples and depicted in Fig. 4. Time $t = 0$ is defined as the start of the movement. The zero values at the start and end of the trajectory allow for pre-actuation and post-actuation, respectively.

4. Overview of techniques

In this section, inversion techniques are presented, developed, and implemented on the benchmark system of section 3.

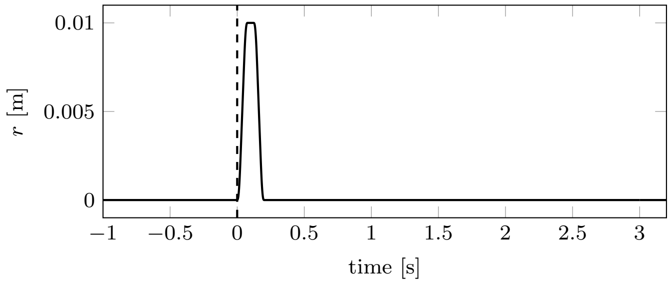

Fig. 4. Reference trajectory r consists of a forward and backward movement and includes pre-actuation and post-actuation time.

Table 2
Overview of NPZ-Ignore, ZPETC and ZMETC for decomposition (2). The DC gain is compensated by $\beta = B_u(1)$, see also Appendix A.

Technique	$F(z)$	Preview	$H(z)F(z)$
NPZ-Ignore	$\frac{A(z)}{\beta B_s(z)}$	$p+d$	$\frac{B_u(z)}{\beta}$
ZPETC	$\frac{z^{-p}A(z)B_u^*(z)}{\beta^2 B_s(z)}$	$p+d$	$\frac{z^{-p}B_u(z)B_u^*(z)}{\beta^2}$
ZMETC	$\frac{A(z)}{B_s(z)B_u^*(z)}$	d	$\frac{B_u(z)}{B_u^*(z)}$

4.1. Approximate inverse (NPZ-Ignore, ZPETC, ZMETC)

4.1.1. Approach

As mentioned in section 2.2, nonminimum-phase zeros and delays are key challenges for system inversion. Let H be decomposed as

$$H(z) = \frac{B_s(z)B_u(z)}{A(z)}, \tag{2}$$

with $B_s(z)$ containing all minimum-phase zeros and $B_u(z)$ the p nonminimum-phase zeros. A key issue is that $(B_u(z))^{-1}$ is unstable. Several techniques have been proposed to approximate the inverse of $B_u(z)$, including NPZ-Ignore [8], zero-phase-error tracking control (ZPETC) [7], and zero-magnitude-error tracking control (ZMETC). The results for these approaches are summarized in Table 2. If $H(z)$ is nonminimum phase, i.e. $p > 0$, then $H(z)F(z) \neq 1$ and stable. If $H(z)$ is minimum phase, i.e. $p = 0$, all three approaches are identical and exact: $H(z)F(z) = 1$. More background on these approaches can be found in Appendix A. See, for example, [10] for a comparison.

4.1.2. Application to benchmark system

To demonstrate the characteristics of these approaches, the approaches are applied to the benchmark system of section 3 for $H = G$. The Bode diagram of HF for each technique is shown in Fig. 5. Recalling that ideally $HF = 1$, it can observed that ZPETC indeed has zero phase error, ZMETC has zero magnitude error, and NPZ-Ignore has both a magnitude and phase error.

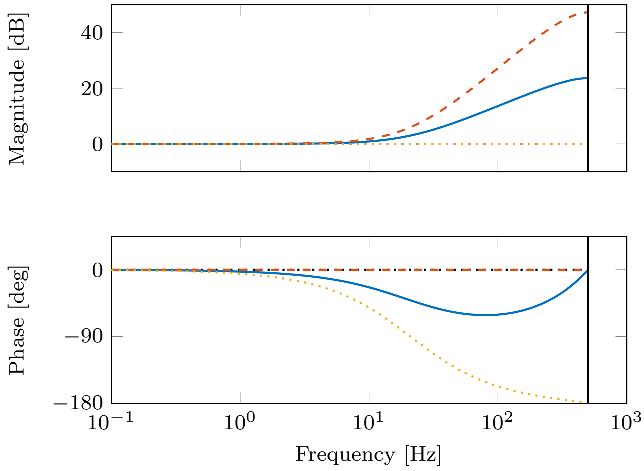

Fig. 5. HF for NPZ-Ignore (——), ZPETC (- - -), and ZMETC (······). HF has zero phase for ZPETC and zero magnitude for ZMETC.

4.1.3. Summary

The techniques in Table 2 are based on an approximate infinite horizon design and have finite preview.

4.2. Stable inversion

In this section, the stable inversion approach for LTI systems is presented. For stable inversion on LTV systems see, for example, [19].

4.2.1. Approach

The techniques presented in the previous section are all based on approximations of the unstable part of the inverse system. In contrast, stable inversion regards the unstable part as a non-causal operation and generates signal u based on infinite preview. Consider LTI system $\bar{H}$ of Remark 1 in state-space form with state x. The state of the inverse $\bar{H}^{-1}$ is divided into a stable and unstable part by applying the state transformation $x[k] = T\begin{bmatrix} x_s[k] \\ x_u[k] \end{bmatrix}$, where T contains eigenvectors of $\bar{H}^{-1}$ such that

$$\begin{bmatrix} x_s[k+1] \\ x_u[k+1] \end{bmatrix} = \begin{bmatrix} A_s & 0 \\ 0 & A_u \end{bmatrix} \begin{bmatrix} x_s[k] \\ x_u[k] \end{bmatrix} + \begin{bmatrix} B_s[k] \\ B_u[k] \end{bmatrix} r[k], \tag{3}$$
$$u[k] = \begin{bmatrix} C_s[k] & C_u[k] \end{bmatrix} \begin{bmatrix} x_s[k] \\ x_u[k] \end{bmatrix} + D[k]r[k],$$

with $|\lambda(A_s)| < 1$ and $|\lambda(A_u)| > 1$, i.e., all stable poles are contained in A_s and all unstable poles in A_u. The states are found through solving

$$x_s[k+1] = A_s x_s[k] + B_s r[k], \quad x_s[-\infty] = 0$$

forward in time and

$$x_u[k+1] = A_u x_u[k] + B_u r[k], \quad x_u[\infty] = 0$$

backward in time. The command signal u follows from

$$u[k] = C_s x_s[k] + C_u x_u[k] + Dr[k].$$

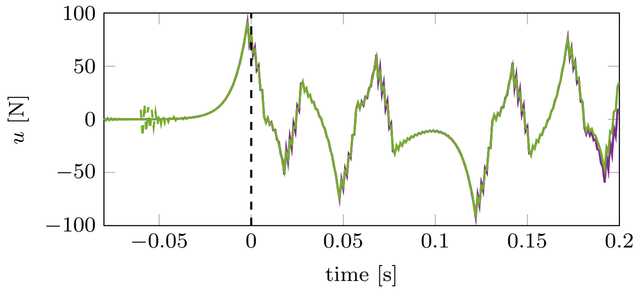

(a) Norm-optimal feedforward, (- - -), (——) generates a non-zero input u at the begin of the task to compensate for boundary effects. The effect is larger for 60 samples preview (- - -) than for 80 samples preview (——). Stable inversion generates identical u with 60 samples preview (- - -) and 80 samples preview (——) for $t \geq -0.06$, whereas for 80 samples preview u is non-zero for $-0.08 \leq t < -0.06$.

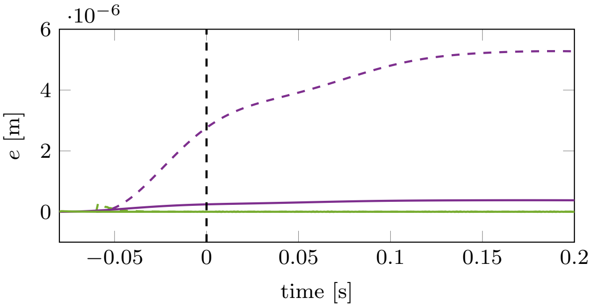

(b) The infinite design of stable inversion (- - -), (——) introduces significant boundary errors on a finite interval, whereas these are much smaller for the finite time design of norm-optimal feedforward (- - -), (——).

Fig. 6. The finite design of norm-optimal feedforward generates an input that compensates for boundary effects and thereby outperforms stable inversion on a finite horizon since the latter is an infinite design.

In practice, the boundaries are finite, i.e., $x_s[0] = 0$, $x_u[N] = x_u^0$, and introduce boundary errors.

The dichotomy in a stable and unstable part as in (3) is nontrivial for linear time varying (LTV) systems. The dichotomy for a very general LTV case is recently presented in [25], namely for linear periodically time varying (LPTV) systems. For the LTI benchmark system considered in this paper the dichotomy can be found through an eigenvalue decomposition as shown above.

4.2.2. Application to benchmark system

To illustrate the influence of preview on the performance of the stable inversion approach, the approach is applied to $H = G$ with r the reference trajectory of Fig. 4 in the time intervals $[-0.06, 0.2]$ and $[-0.08, 0.2]$, i.e., the pre-actuation is restricted to either 60 or 80 samples and the post-actuation to 0 samples. The results shown in Fig. 6 show a considerable performance improvement when increasing the pre-actuation from 60 to 80 samples. For infinite pre-actuation and post-actuation, the results become exact.

4.2.3. Summary

Stable inversion is an infinite time design that is exact on an infinite time horizon and has infinite preview. A finite time horizon introduces boundary errors.

4.3. Norm-optimal feedforward/ILC

In this section, norm-optimal inversion techniques based on norm-optimal ILC techniques are considered.

4.3.1. Approach

Within ILC there are two main classes [3]. The first class is frequency domain ILC in which a learning filter $L \approx (SG)^{-1}$ is constructed. The filter is typically implemented using ZPETC or ZMETC, see section 4.1. The second class is norm-optimal ILC in which the 2-norms of e_{j+1} and f_{j+1} are minimized. Here, subscript j denotes the current trial and $j{+}1$ the next trial. Common solution methods are adjoint ILC and lifted ILC. The reader is referred to [26, 27] for adjoint ILC, including the effect of nonminimum-phase zeros. In this paper the focus is on lifted ILC. In lifted ILC the solution is based on describing input-output relations in lifted/supervector notation [28]. For example, the relation between y and u is described by

$$\underbrace{\begin{bmatrix} y[0] \\ y[1] \\ \vdots \\ y[N{-}1] \end{bmatrix}}_{\underline{y}} \underbrace{\begin{bmatrix} h[0] & 0 & \dots & 0 \\ h[1] & h[0] & \dots & 0 \\ \vdots & \vdots & \ddots & \vdots \\ h[N{-}1] & h[N{-}2] & \dots & h[0] \end{bmatrix}}_{\underline{H}} \underbrace{\begin{bmatrix} u[0] \\ u[1] \\ \vdots \\ u[N{-}1] \end{bmatrix}}_{\underline{u}},$$

where $\underline{h}$ is the impulse response of H given by

$$h[k] = \begin{cases} D, & k = 0, \\ CA^{k-1}B, & k = 1, 2, \dots, N, \end{cases}$$

with N the task length. A general performance criterion is

$$\|e_{j+1}\|^2_{\underline{W}_e} + \|f_{j+1}\|^2_{\underline{W}_f} + \|f_{j+1} - f_j\|^2_{\underline{W}_{\Delta f}}, \tag{4}$$

where $\|(\cdot)\|^2_W = (\cdot)^\top W(\cdot)$, with $\underline{W}_e = w_e \underline{I}_N$, $\underline{W}_f = w_f \underline{I}_N$, $\underline{W}_{\Delta f} = w_{\Delta f} \underline{I}_N$. The solution that minimizes this criterion is, see for example [19, Theorem 2],

$$\begin{aligned} \underline{f}_{j+1} &= \underline{Q}\,\underline{f}_j + \underline{L}\,\underline{e}_j, \\ \underline{Q} &= \left(\underline{H}^\top w_e \underline{H} + w_f \underline{I} + w_{\Delta f} \underline{I}\right)^{-1} \left(\underline{H}^\top w_e \underline{H} + w_{\Delta f} \underline{I}\right), \\ \underline{L} &= \left(\underline{H}^\top w_e \underline{H} + w_f \underline{I} + w_{\Delta f} \underline{I}\right)^{-1} \underline{H}^\top w_e. \end{aligned}$$

The use of $N \times N$ matrix calculations results in extensive computation times growing as $\mathcal{O}(N^3)$ [19]. An alternative is to use Riccati equations to find the optimal solution as is done in [19]. The approach yields exactly the same optimal solution, but the computation time is limited to $\mathcal{O}(N)$. Next, the resource-efficient approach based on Riccati equations is used for both ILC and feedforward design.

First, the approach for ILC is presented. Criterion (4) is equivalent to

$$\sum_{k=1}^{N-1}\Big((e_{j+1}[k])^\top w_e(e_{j+1}[k]) + (f_{j+1}[k])^\top w_f(f_{j+1}[k]) + (f_{j+1}[k]-f_j[k])^\top w_{\Delta f}(f_{j+1}[k]-f_j[k])\Big). \tag{5}$$

The optimal command signal f_{j+1} that minimizes (5) is the output of the state-space system

$$\left[\begin{array}{c|ccc} A-BL[k] & -BL_f[k] & BL_e[k] & BL_g[k] \\ \hline -L[k] & I_{n_i}-L_f[k] & L_e[k] & L_g[k] \end{array}\right],$$

with zero initial state for input $\begin{bmatrix} f_j[k] \\ e_j[k] \\ g_{j+1}[k+1] \end{bmatrix}$, where

$$\begin{aligned} L[k] &= \left(\gamma^{-1}[k] + B^\top P[k+1]B\right)^{-1} \\ &\qquad \times \left(D^\top w_e C + B^\top P[k+1]A\right), \\ L_f[k] &= \left(\gamma^{-1}[k] + B^\top P[k+1]B\right)^{-1} w_f, \\ L_e[k] &= \left(\gamma^{-1}[k] + B^\top P[k+1]B\right)^{-1} D^\top w_e, \\ L_g[k] &= \left(\gamma^{-1}[k] + B^\top P[k+1]B\right)^{-1} B^\top, \\ \gamma &= \left(D^\top w_e D + w_f + w_{\Delta f}\right)^{-1}, \end{aligned}$$

with

$$\begin{aligned} g_{j+1}[k] &= \left(A^\top - K_g[k]B^\top\right) g_{j+1}[k+1] + C^\top w_e e_j[k] \\ &\qquad + K_g[k] w_f f_j[k], \\ g_{j+1}[N] &= 0_{n_x\times 1}, \end{aligned}$$

where

$$\begin{aligned} K_g[k] &= \left(A^\top - C^\top w_e D\gamma B^\top\right) P[k+1] \\ &\qquad \times \left(I_{n_x} + B\gamma B^\top P[k+1]\right)^{-1} B\gamma, \end{aligned}$$

and $P[k]$ the solution of the matrix difference Riccati equation

$$\begin{aligned} P[k] &= \left(A - B\gamma D^\top w_e C\right)^\top P[k+1] \\ &\quad \times \left(I_{n_x} - B\left(\gamma^{-1}[k] + B^\top P[k+1]B\right)^{-1} B^\top P[k+1]\right) \\ &\quad \times \left(A - B\gamma D^\top w_e C\right) \\ &\quad + C^\top w_e C - (D^\top w_e C)^\top \gamma (D^\top w_e C), \\ P[N] &= 0_{n_x\times n_x}. \end{aligned}$$

It can be shown that $\|e_j - e_\infty\|_2$ converges monotonically if $w_e > 0$, $w_f, w_{\Delta f} \geq 0$. If H is strictly proper (i.e., $D = 0$), then $w_f > 0$ or $w_{\Delta f} > 0$ is required to guarantee monotonic convergence. This inherently reduces the performance in terms of $\|e\|_2$ since input f_j is penalized. To avoid this, H can be made bi-proper by applying time-shifts (see Remark 1) such that $D \neq 0$ and hence $w_f = w_{\Delta f} = 0$ can be used.

Next, the approach for inverse model feedforward is presented. Feedforward can be seen as a special case of ILC in which there is only one trial and hence no input change weight $w_{\Delta f}$. In particular, if H is bi-proper and $w_f, w_{\Delta f} = 0$, the solution reduces to inverse model ILC. Without input change weight ($w_{\Delta f} = 0$), and $w_e = Q$, $w_f = R$, (5) reduces to the LQ criterion

$$\sum_{k=1}^{N-1}(e[k])^\top Q(e[k]) + (u[k])^\top R(u[k]).$$

For the case without direct feedthrough ($D = 0$), the problem reduces to the well-known LQ tracking problem [15], with solution

$$\begin{aligned} x[k+1] &= (A - BL[k])x[k] + BL_g[k]g[k+1], \quad x[0] = 0, \\ u[k] &= -L[k]x[k] + L_g[k]g[k+1], \end{aligned}$$

where

$$\begin{aligned} L[k] &= \left(R + B^\top P[k+1]B\right)^{-1} B^\top P[k+1]A, \\ L_g[k] &= \left(R + B^\top P[k+1]B\right)^{-1} B^\top, \end{aligned}$$

with

$$\begin{aligned} g[k] &= C^\top Q r[k] + \\ &\quad A^\top\left(I - (P^{-1}[k+1] + BR^{-1}B^\top)^{-1}BR^{-1}B^\top\right) g[k+1], \\ g[N] &= 0, \end{aligned}$$

and $P[k]$ the solution of the matrix difference Riccati equation

$$\begin{aligned} P[k] &= C^\top QC + A^\top P[k+1]A \\ &\quad - A^\top P[k+1]B\left(R + B^\top P[k+1]B\right)^{-1} B^\top P[k+1]A, \\ P[N] &= 0. \end{aligned}$$

4.3.2. Application to benchmark system

The norm-optimal feedforward approach is applied to the benchmark system $H = G$ under the same conditions as in section 4.2, i.e., with reduced pre-actuation and post-actuation. The results are shown in Fig. 6. The approach outperforms stable inversion since it takes the boundary effects into account using the linear time varying (LTV) character of the solution. This behavior can be observed at the start of u in Fig. 6(a).

4.3.3. Summary

Norm-optimal ILC/feedforward is a finite time design and has infinite preview (equal to the task length). The approach is optimal in terms of minimizing $\|e\|_2$ if $w_f = 0$ in ILC or if $R = 0$ in feedforward.

4.4. Preview control

In preview control the inverse system is optimized for a specific infinite time objective, with pre-defined preview.

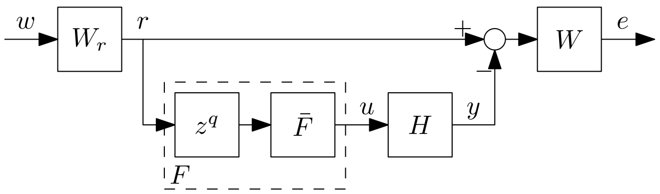

(a) In preview control the objective is minimization of a certain norm x on the transfer $w \to e$.

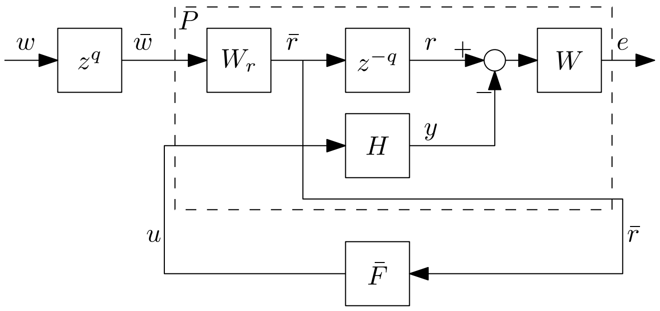

(b) General plant formulation.

Fig. 7. In preview control the preview q is fixed and $\bar{F}$ is optimized to minimize a certain norm on the transfer $\bar{w} \to e$.

4.4.1. Approach

A general formulation of preview control is shown in Fig. 7(a) where F is decomposed into $F = \bar{F} z^q$, with preview $q \in \mathbb{N}$. Note that an input weighting W_r is added compared to Fig. 1(c). For fixed q, $\bar{F}$ follows from

$$\bar{F} = \arg\min_{\bar{F}} \|W\left(z^{-q} - H\bar{F}\right) W_r\|_x, \tag{6}$$

where x is a certain norm. The problem cast into the general plant formulation is shown in Fig. 7(b). Note that the pre-multiplication with the a-causal part z^q is not part of generalized plant P to ensure $P \in \mathcal{RH}_\infty$. For the special case without preview (i.e., $q = 0$), the approach in [17] is recovered.

First, optimal ILC synthesis is presented in which the induced (worst-case) 2-norm of the error e is minimized by using $\mathcal{H}_\infty$ preview control, i.e., $x = \infty$ in (6). The input is set to $w = r$, i.e., $W_r = 1$. $\mathcal{H}_\infty$-synthesis on P minimizes $\|W\left(z^{-q} - H\bar{F}\right)\|_\infty = \|W\left(1 - HF\right)\|_\infty$ which is the ILC convergence criterion if $W = 1$, see also section 2.3.

Second, optimal inverse model feedforward synthesis is presented in which $\|e\|_2$ is minimized for a specific reference r by using $\mathcal{H}_2$ preview control, i.e., $x = 2$ in (6). Input w is white noise of unity intensity and W_r is the power spectrum of r such that $\mathcal{H}_2$-synthesis on P minimizes $\|e\|_2$ for the spectrum of $r = W_r w$.

4.4.2. Application to benchmark system

For $\mathcal{H}_\infty$-preview control in a feedfoward setting, the results for a range of preview values q are shown in Fig. 8(a). More preview q introduces more design freedom and hence $\|W(1 - HF)\|_\infty$ decreases.

For $\mathcal{H}_2$-preview control in a feedforward setting with

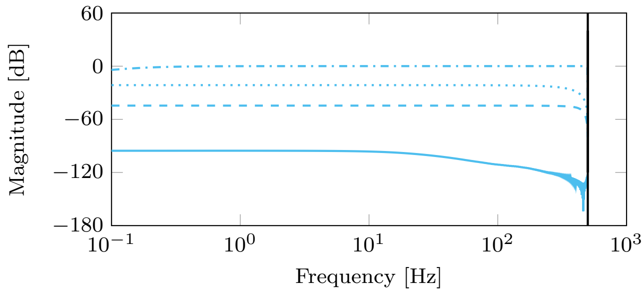

(a) $W(1 - HF)$ for $\mathcal{H}_\infty$ preview control for $q = 0$ (-·-·-), $q = 20$ (·····), $q = 40$ (- - -), and $q = 90$ (——). For larger q, the maximum magnitude $|W(1 - HF)|$ is smaller.

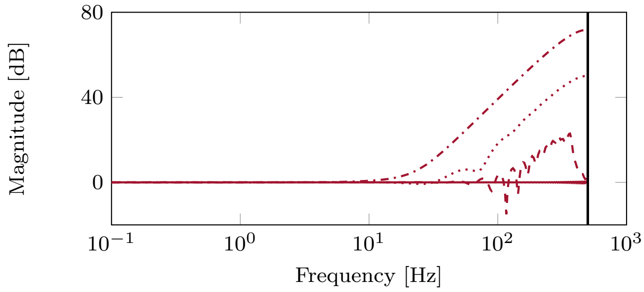

(b) HF for $\mathcal{H}_2$ preview control for $q = 1$ (-·-·-), $q = 20$ (·····), $q = 40$ (- - -), and $q = 90$ (——). For larger q, $|HF|$ is closer to unity.

Fig. 8. $\mathcal{H}_\infty$ and $\mathcal{H}_2$ preview control for a range of preview values q. More preview yields higher performance.

input weighting

$$W_r(z) = \left(\frac{2.0236(z + 0.03295)}{z - 0.9570}\right)^4, \tag{7}$$

the resulting filters HF for a range of preview values q are shown in Fig. 8(b). For larger q, $|HF|$ is closer to unity.

4.4.3. Summary

Preview control is an infinite time design with finite predefined preview. $\mathcal{H}_\infty$ and $\mathcal{H}_2$ preview control address the control goal in ILC and feedforward, respectively.

5. A control goal perspective

A qualitative overview of the inversion techniques of the previous section is provided in Table 3. Extensions to multivariable and time varying systems are presented in section 7. In this section, the control goal is added to the inversion techniques of section 4 and the results are validated on the benchmark system of section 3.

5.1. Application to feedforward

Table 4 summarizes the results of the techniques in a feedforward setting on the benchmark system of section 3. For norm-optimal feedforward the system is made bi-proper through shifting r such that $R = 0$ can be used, see also section 4.3. For $\mathcal{H}_\infty$ and $\mathcal{H}_2$ preview control

Table 3
Overview of inversion techniques. *see section 7.

Technique	Design	Preview	Dimensions*	Time varying*	Aim
NPZ-Ignore	Infinite	Finite	SISO	No	H^{-1} approximation
ZPETC	Infinite	Finite	SISO	No	H^{-1} approximation
ZMETC	Infinite	Finite	SISO	No	H^{-1} approximation
Stable inversion	Infinite	Infinite	Square	Yes	H^{-1} exact
Norm-optimal	Finite	Infinite	Non-square	Yes	$\min \|e\|_2$
$\mathcal{H}_\infty$ preview	Infinite	Finite	Non-square	No	$\min \|W(1-HF)\|_\infty$
$\mathcal{H}_2$ preview	Infinite	Finite	Non-square	No	$\min \|e\|_2$

Table 4
Design and performance in a feedforward setting.

Technique	Settings	$\|e\|_2$
NPZ-Ignore	-	0.0153
ZPETC	-	0.0050
ZMETC	-	0.0317
Stable inversion	-	3.5849×10^{-11}
Norm-optimal	$Q=1$; $R=0$	7.7392×10^{-11}
$\mathcal{H}_\infty$ preview	$q=100$	3.6942×10^{-6}
$\mathcal{H}_2$ preview	W_r: (7); $q=100$	6.6786×10^{-9}

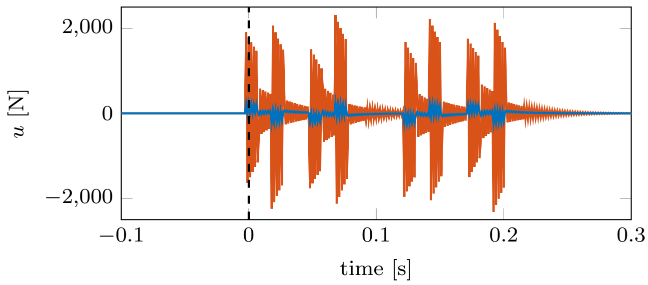

(a) NPZ-Ignore (—) and ZPETC (—).

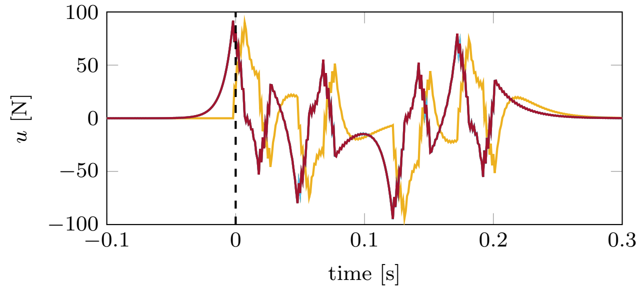

(b) ZMETC (—), stable inversion (—), norm-optimal feedforward (—), $\mathcal{H}_\infty$ preview control (—), and $\mathcal{H}_2$ preview control (—).

Fig. 9. Command signal u. The signals in (a) are unacceptably large. The signals in (b) are satisfactory.

$q = 100$ samples preview are used. W_r for $\mathcal{H}_2$ preview control is given by (7).

The time signals u, e are shown in Fig. 9 and Fig. 10, respectively. Fig. 9 shows $d = 1$ sample preview for ZMETC, $p + d = 2$ samples preview for NPZ-Ignore and ZPETC, $q = 100$ samples preview for $\mathcal{H}_\infty$ preview control and $\mathcal{H}_2$ preview control, and infinite preview for stable inversion and norm-optimal feedforward.

Fig. 9(a) shows that the generated inputs of NPZ-Ignore and ZPETC are not very well suited for practical application, which is in line with the analysis in [10, Section 6]. Also the errors are considerably large as shown in Table 4 and Fig. 10. Note that only part of the time axis is shown.

Fig. 9(b) shows that the inputs of stable inversion, norm-optimal feedforward, $\mathcal{H}_\infty$ preview control, and $\mathcal{H}_2$ preview control are similar, whereas that of ZMETC is different. Table 4 and Fig. 10 show a large error for the approximate inverse techniques. Stable inversion, norm-optimal feedforward, and $\mathcal{H}_2$ preview control achieve the lowest $\|e\|_2$, which is to be expected since these techniques are aimed at minimizing $\|e\|_2$, see also Table 3. $\mathcal{H}_\infty$ preview control achieves moderate performance since it aims at minimizing $\min \|W(1-HF)\|_\infty$ rather than $\|e\|_2$. The desired preview in preview control depends on the location of the nonminimum-phase zeros [29], where higher preview enhances performance.

5.2. *Application to ILC*

5.2.1. *Guaranteed convergence*

In an ILC setting, there is guaranteed convergence in error norm $\|e_j\|_2$ over the trials if $\|W(1-HF)\|_\infty = \|1-GSF\|_\infty < 1$, see also section 2.3. It might be possible that the condition cannot be satisfied at all, but if the condition can be satisfied, $\mathcal{H}_\infty$ preview control guarantees convergence since it minimizes $\|W(1-HF)\|_\infty$, see section 4.4. Fig. 11(a) shows the Bode magnitude $|W(1-HF)|$ for techniques with explicit design of F. Note that since the benchmark system is singlevariable, $\|W(1-HF)\|_\infty = \max_\omega |W(e^{j\omega h})(1-H(e^{j\omega h})F(e^{j\omega h}))|$. The figure reveals that both $\mathcal{H}_\infty$ preview control and $\mathcal{H}_2$ preview control are guaranteed to converge. The approximate inverse techniques require a robustness filter $W \neq 1$ to guarantee convergence, which goes at the expense of performance, i.e., $W(1-HF)$ for some possibly noncausal W.

On an infinite time horizon, stable inversion is also guaranteed to converge since it is exact. However, on a finite time interval truncation errors might deteriorate conver-

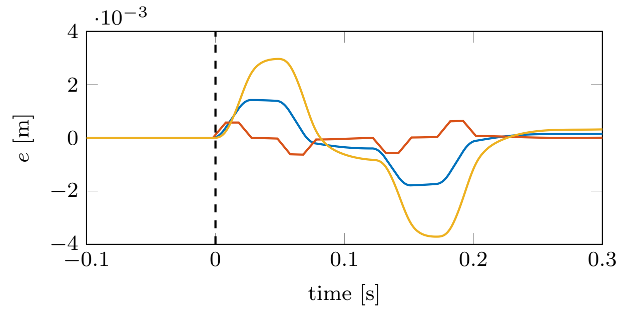

(a) NPZ-Ignore (—), ZPETC (—), and ZMETC (—).

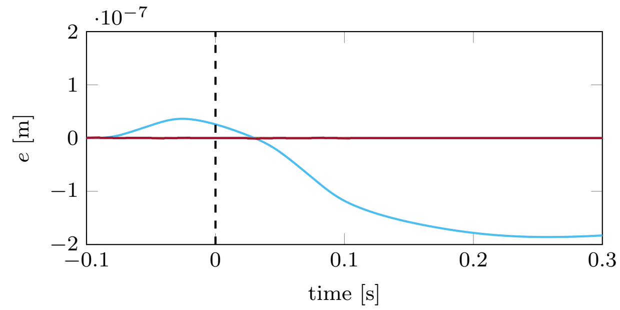

(b) Stable inversion (—), norm-optimal feedforward (—), $\mathcal{H}_\infty$ preview control (—), and $\mathcal{H}_2$ preview control (—). Norm-optimal, stable inversion, and $\mathcal{H}_2$ preview are overlapping.

Fig. 10. Error signal e. The errors in (a) are unacceptably large. The errors in (b) are close to zero as desired.

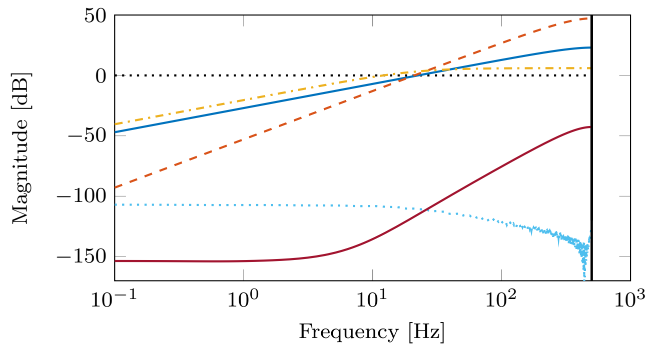

(a) ILC convergence is only guaranteed for $\mathcal{H}_\infty$ preview control (⋯) and $\mathcal{H}_2$ preview control (—) since only for these approaches $|1 - GS(e^{j\omega h})F(e^{j\omega h})| < 1$, for all frequencies ω. The approximate inverse techniques NPZ-Ignore (—), ZPETC (- - -), and ZMETC (-·-) require an additional robustness to guarantee convergence (not shown).

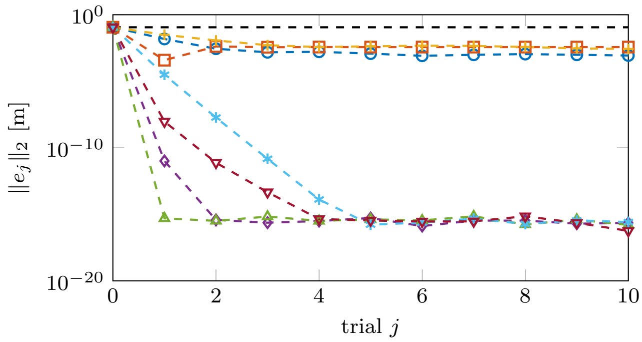

(b) For the approximate inverse techniques NPZ-Ignore (—o—), ZPETC (—□—), and ZMETC (—+—) convergence is enforced through a robustness filter $W = Q^*Q$ at the cost of performance $\|e_j\|_2$. All other techniques, i.e., stable inversion (—◆—), norm-optimal feedforward (—▲—), $\mathcal{H}_\infty$ preview control (—*—), and $\mathcal{H}_2$ preview control (—▽—), converge to zero error up to numerical precision. Norm-optimal ILC is exact and therefore converges in a single trial.

Fig. 11. Application in ILC with the convergence condition in (a) and the performance in (b).

gence. Finally, convergence can be guaranteed for norm-optimal ILC by proper weight selection, see section 4.3.

In summary, convergence in $\|e_j\|_2$ can be guaranteed for $\mathcal{H}_\infty$ preview control, $\mathcal{H}_2$ preview control, norm-optimal ILC, and stable inversion (on an infinite horizon). For NPZ-Ignore, ZPETC and ZMETC an additional robustness filter $W \neq 1$ is required to enforce convergence, at the cost of performance.

5.2.2. Application to the benchmark system

The convergence on the benchmark system of section 3 is investigated. Fig. 11(b) shows $\|e_j\|_2$ over 11 trials. The results show that there is indeed convergence for $\mathcal{H}_\infty$ preview control, $\mathcal{H}_2$ preview control, and norm-optimal ILC, and also for stable inversion despite the boundary errors. For the approximate inverse techniques NPZ-Ignore, ZPETC, and ZMETC an additional robust filter W is used to guarantee convergence. The robustness filter is designed as $W = Q^*Q$ with Q^* the adjoint of Q to avoid phase distortion. A first-order low-pass filter is used for Q to reduce the high frequent magnitude, see also Fig. 11(a).

Since the approximate inverse techniques NPZ-Ignore, ZPETC, and ZMETC require an additional robustness filter $W \neq 1$, the limit error is nonzero, i.e., $e_\infty \neq 0$. The consequence is a poor performance as shown by Figure 11(b) confirming statements in earlier sections.

Since there are no trial-varying disturbances, the theoretical limit error equals $e_\infty = 0$ for all methods without robustness filter, i.e., all except the approximate inverse techniques. However, due to numerical aspects, this value it not achieved exactly. Norm-optimal ILC converges in a single trial to e_∞ since $w_f = w_{\Delta f} = 0$. In contrast, $\mathcal{H}_\infty$ preview control, $\mathcal{H}_2$ preview control and stable inversion are not exact and therefore require multiple trials to converge. The number of preview samples q in $\mathcal{H}_\infty$ preview control ($q = 100$ in Fig. 11) directly influences the convergence speed. Ideally, the $\mathcal{H}_2$ preview control filter F is updated every trial based on the spectrum of e_j. Fig. 11 shows the results for fixed F based on the spectrum of $e_0 = Sr$ with $q = 100$.

6. Non-square systems

In the preceding sections, several inversion techniques are developed that include preview. Essentially, there are two reasons for preview: strict delays, which is quite obvious, and nonminimum-phase zeros. An interesting observation is that such nonminimum-phase zeros are essentially the values z where

$$\left[\begin{array}{c|c} zI-A & -B \\ \hline C & D \end{array}\right] \tag{8}$$

loses rank. As a result, in general a non-square system will have no zeros and hence also no nonminimum-phase zeros. However, direct inversion using (1) is not possible since D is not invertible. Depending on the excess of inputs or outputs, infinitely many or no exact solution exists. In this section, an approach is developed that allows for causal inversion of general nonminimum-phase systems.

6.1. A squaring-down approach

For systems with more inputs than outputs, system F in Fig. 1(c) is composed as $F = T_u\tilde{F}$. First, transformation T_u is constructed such that HT_u is square. The transformation T_u is generally dynamic but can also be static, i.e., independent of frequency. Techniques for squaring down can be found in, for example, [30, 31, 32]. Second, $\tilde{F}$ is obtained through inversion of HT_u using (1). In certain cases, a T_u exists such that the squared-down system is minimum phase. Such a transformation enables exact inversion and avoids the use of preview.

Systems with more outputs than inputs are the dual of systems with more inputs than outputs.

6.2. Application to benchmark system

The procedure is applied to the two-input, single-output system of Fig. 12(a). The system is an extended version of the benchmark system in Fig. 2, with the addition of input u_2 located $0.1l$ from input u_1. The system H from $\begin{bmatrix} u_1 & u_2 \end{bmatrix}^\top \to y$ is given by

$$\left[\begin{array}{c|cc} A & B_1 & B_2 \\ \hline C & D_1 & D_2 \end{array}\right] =$$

$$\left[\begin{array}{cccc|cc} 1.0000 & 0.0010 & 0 & 0 & 0.0000 & 0.0000 \\ 0 & 1.0000 & 0 & 0 & 0.0001 & 0.0001 \\ 0 & 0 & 0.9981 & 0.0010 & 0.0000 & 0.0000 \\ 0 & 0 & -3.6783 & 0.9614 & 0.0037 & 0.0029 \\ \hline 1.0000 & 0 & -0.0500 & 0 & 0 & 0 \end{array}\right].$$

By (8) it follows that the transfer $u_1 \to y$, i.e., (A, B_1, C, D_1) has a nonminimum-phase zero at $z = 1.140$ (see also section 3) and that the transfer $u_2 \to y$, i.e., (A, B_2, C, D_2), has a nonminimum-phase zero at $z = 1.2965$. Since both transfers have a single nonminimum-phase zero, the step responses of both initially move in opposite direction [24], see Fig. 12(c). Because the nonminimum-phase zeros are different, non-square H is minimum phase.

The static transformation

$$T_u = \begin{bmatrix} -1 \\ 1.1 \end{bmatrix} \tag{9}$$

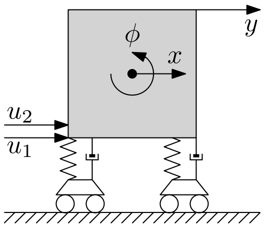

(a) Both tranfers $u_1 \to y$ and $u_2 \to y$ are non mininimum phase.

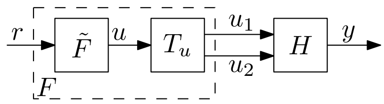

(b) Transformation T_u down-squares H to a single-input, single-output system HT_u.

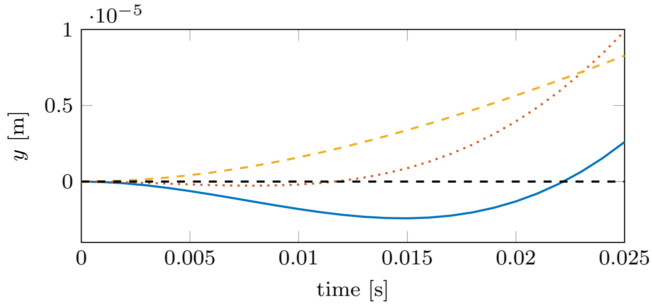

(c) The step responses of the transfers $u_1 \to y$ (——) and $u_2 \to y$ (······) initially move in opposite direction of the final value, confirming nonminimum-phase behavior. The step response of the down-squared system (– – –) moves in the direction of the final value, confirming minimum-phase behavior.

Fig. 12. The two-input, single-output system, with both transfers nonminimum phase, is down-squared to a single-input, single-output, minimum-phase system.

yields the single-input, single-output system $HT_u \stackrel{s}{=} (A, \begin{bmatrix} B_1 & B_2 \end{bmatrix} T_u, C, \begin{bmatrix} D_1 & D_2 \end{bmatrix} T_u)$, where

$$\begin{bmatrix} B_1 & B_2 \end{bmatrix} T_u = 10^{-3} \times \begin{bmatrix} 0.0000 \\ 0.0125 \\ -0.0002 \\ -0.4414 \end{bmatrix}.$$

Through (8) it can be shown that HT_u has no nonminimum-phase zeros, which is confirmed by the step response in Fig. 12(c).

Direct inversion (1) on square, minimum-phase HT_u yields $\tilde{F}$. The inputs u_1, u_2 are shown in Fig. 13. Note that since HT_u is strictly proper with relative degree $d = 1$, one sample preview is required, see also Remark 1.

6.3. Summary

The results confirm that additional actuators and sensors are very promising, also in the field of inversion and learning control, especially when nonminimum-phase zeros are encountered. This strongly relates to recent research on overactuation and oversensing, see [33] in this respect.

Here, a two-step approach is outlined. First, the system is down-squared using static or dynamic transformations. Second, exact inversion is used, avoiding the need for preview.

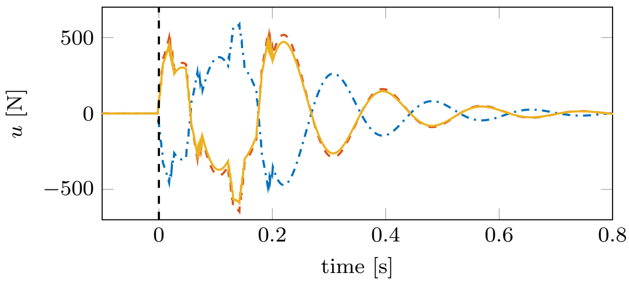

Fig. 13. For the two-input, single-output system of Fig. 12, the transformation (9) enables the use of exact and direct inversion (1) yielding bounded inputs u_1 (-·-·), u_2 (- - -), and combined input u (——).

The results also impact, e.g., the preview control approaches in section 4.4, where it will lead to much less required preview. Hence, one can also use these optimization based approaches. The present experience reveals that these have much better results with more inputs and/or outputs, since a much larger design freedom can be exploited.

7. Extensions: multivariable, time varying, parameter-varying, and nonlinear

The applicability of each technique to multivariable and time varying systems is summarized in Table 3. For NPZ-Ignore, ZPETC, and ZMETC the extension to multivariable systems is nontrivial. In [20], an approach for multivariable ZPETC is proposed which applies multiple times SISO ZPETC to the Smith form of the system. Similarly, the Smith form can be used to construct NPZ-Ignore and ZMETC. However, in [20] it is concluded that at present there are no numerically stable algorithms for finding Smith forms. Therefore, these techniques currently seem to be limited to SISO systems.

Techniques based on state-space descriptions, such as stable inversion and norm-optimal feedforward/ILC, can directly be extended to multivariable systems. Note, however, that stable inversion is only applicable to square systems since it requires the inverse system (1). Also $\mathcal{H}_\infty$ and $\mathcal{H}_2$ preview control can directly be extended, but the exact implementation depends on the specific requirements. For example, in ILC convergence over trials of the error e_j is determined by $(I - (GS)F)$ whereas convergence of input u is determined by $(I - F(GS))$, and generally $F(GS) \neq (GS)F$ for multivariable systems. For underactuated systems, i.e., with more outputs than inputs, exact tracking is impossible. For overactuated systems, i.e., with more inputs than outputs, exact tracking is possible and the additional degrees of freedom can be exploited to satisfy additional requirements, see for example the approach in section 6.

Application to time varying systems is restricted to the finite time design techniques stable inversion and norm-optimal feedforward/ILC since others are based on time invariant frequency domain techniques. However, the dichotomy in stable inversion is nontrivial for general time varying systems. For linear periodically time varying (LPTV) systems this is solved in [25].

For stable inversion for nonlinear systems, the reader is referred to [34, 35]. For linear parameter-varying systems, the reader is referred to [36].

8. Conclusion and outlook

Inversion techniques are essential for achieving high performance in motion systems, either through inverse model feedforward or learning control. In this paper, the criteria for inverse model feedforward and ILC are posed and several inversion techniques are investigated, developed, and compared on a nonminimum-phase benchmark system, resulting in the following guidelines.

For inverse model feedforward, norm-optimal feedforward (section 4.3) has important advantages as it explicitly takes into account boundary effects. If boundary effects are not critical, $\mathcal{H}_2$ preview control (section 4.4) is recommended as infinite time design.

For ILC, filter synthesis via $\mathcal{H}_\infty$ preview control (section 4.4) is strongly recommended, since the optimization criterion is taken equal to the convergence condition of ILC. For non-optimal filter design, stable inversion (section 4.2) is experienced to yield better results than the approximate inverse techniques NPZ-Ignore, ZPETC, and ZMETC (section 4.1). Importantly, the approximate inverse techniques typically require an additional robustness filter at the cost of performance.

For applicability of the techniques to multivariable and time varying systems the following conclusions are drawn. The approximate inverse techniques NPZ-Ignore, ZPETC, and ZMETC are currently limited to SISO systems. Stable inversion, norm-optimal feedforward/ILC, $\mathcal{H}_\infty$ preview control, and $\mathcal{H}_2$ preview control can directly be applied multivariable systems, though stable inversion is limited to square systems. Only stable inversion and norm-optimal feedforward/ILC are applicable to time varying systems.

Ongoing research focuses on different system classes such as linear time-varying (LTV), linear periodically time-varying (LPTV), linear parameter varying (LPV), position-dependent, and data-driven methods [37, 21, 38, 39]. Results will be reported elsewhere.

Acknowledgments

The authors would like to acknowledge Sander Verhoeven, Janno Lunenburg, Lennart Blanken, and Robin de Rozario for their early contributions to the presented research.

References

[1] F. Boeren, A. Bareja, T. Kok, T. Oomen, Frequency-Domain ILC Approach for Repeating and Varying Tasks: With Ap-

plication to Semiconductor Bonding Equipment, IEEE/ASME Transactions on Mechatronics 21 (6) (2016) 2716–2727.
[2] M. Steinbuch, R. van de Molengraft, Iterative learning control of industrial motion systems, in: Proceedings of 1st IFAC Conference on Mechatronic Systems, Darmstadt, Germany, 2000, pp. 967–972.
[3] D. Bristow, M. Tharayil, A. Alleyne, A Survey of Iterative Learning Control, Control Systems Magazine 26 (3) (2006) 96–114.
[4] F. Boeren, T. Oomen, M. Steinbuch, Iterative motion feedforward tuning: A data-driven approach based on instrumental variable identification, Control Engineering Practice 37 (2015) 11–19.
[5] L. M. Silverman, Inversion of Multivariable Linear Systems, Transactions on Automatic Control 14 (3) (1969) 270–276.
[6] M. Tomizuka, Optimal Continuous Finite Preview Problem, Transactions on Automatic Control 20 (3) (1975) 362–365.
[7] M. Tomizuka, Zero Phase Error Tracking Algorithm for Digital Control, Journal of Dynamic Systems, Measurement, and Control 109 (1) (1987) 65–68.
[8] E. Gross, M. Tomizuka, W. Messner, Cancellation of discrete time unstable zeros by feedforward control, Journal of Dynamic Systems, Measurement, and Control 116 (1) (1994) 33–38.
[9] D. Torfs, J. De Schutter, J. Swevers, Extended Bandwidth Zero Phase Error Tracking Control of Nonminimal Phase Systems, Journal of Dynamic Systems, Measurement, and Control 114 (3) (1992) 347–351.
[10] J. Butterworth, L. Pao, D. Abramovitch, Analysis and comparison of three discrete-time feedforward model-inverse control techniques for nonminimum-phase systems, Mechatronics 22 (5) (2012) 577–587.
[11] C. Wang, M. Zheng, Z. Wang, M. Tomizuka, Robust Two-Degree-of-Freedom Iterative Learning Control for Flexibility Compensation of Industrial Robot Manipulators, in: International Conference on Robotics and Automation, Stockholm, Sweden, 2016, pp. 2381–2386.
[12] D. de Roover, O. H. Bosgra, Synthesis of robust multivariable iterative learning controllers with application to a wafer stage motion system, International Journal of Control 73 (10) (2000) 968–979.
[13] A. Hazell, D. J. Limebeer, An efficient algorithm for discrete-time H_∞ preview control, Automatica 44 (9) (2008) 2441–2448.
[14] L. Mirkin, On the H_∞ fixed-lag smoothing: how to exploit the information preview, Automatica 39 (8) (2003) 1495–1504.
[15] M. Athans, P. L. Falb, Optimal Control - An Introduction to the Theory and Its Applications, McGraw-Hill Inc., New York, 1966.
[16] S. Gunnarsson, M. Norrlöf, On the design of ILC algorithms using optimization, Automatica 37 (12) (2001) 2011–2016.
[17] J. T. Wen, B. Potsaid, An Experimental Study of a High Performance Motion Control System, in: Proceedings of the 2004 American Control Conference, Boston, Massachusetts, 2004, pp. 5158–5163.
[18] D. A. Bristow, K. L. Barton, A. G. Alleyne, Iterative Learning Control, in: W. S. Levine (Ed.), The Control Systems Handbook: Control System Advanced Methods, 2nd Edition, CRC Press, 2010, Ch. 36, pp. 1–19.
[19] J. van Zundert, J. Bolder, S. Koekebakker, T. Oomen, Resource-efficient ILC for LTI/LTV systems through LQ tracking and stable inversion: Enabling large feedforward tasks on a position-dependent printer, Mechatronics 38 (2016) 76–90.
[20] L. Blanken, J. Willems, S. Koekebakker, T. Oomen, Design Techniques for Multivariable ILC: Application to an Industrial Flatbed Printer, in: Proceedings of the 7th IFAC Symposium on Mechatronic Systems, Loughborough, UK, 2016, pp. 213–221.
[21] K.-T. Teng, T.-C. Tsao, A comparison of Inversion Based Iterative Learning Control Algorithms, in: Proceedings of the 2015 American Control Conference, Chicago, Illinois, 2015, pp. 3564–3569.
[22] S. Devasia, Output Tracking with Nonhyperbolic and Near Nonhyperbolic Internal Dynamics: Helicopter Hover Control, in: Proceedings of the 1997 American Control Conference, Vol. 3, Albuquerque, New Mexico, 1997, pp. 1439–1446.
[23] S. H. van der Meulen, R. L. Tousain, O. H. Bosgra, Fixed Structure Feedforward Controller Design Exploiting Iterative Trials: Application to a Wafer Stage and a Desktop Printer, Journal of Dynamic Systems, Measurement, and Control 130 (5) (2008) 051006:1–16.
[24] M. Vidyasagar, On Undershoot and Nonminimum Phase Zeros, Transactions on Automatic Control 31 (5) (1986) 440.
[25] J. van Zundert, T. Oomen, An Approach to Stable Inversion of LPTV Systems with Application to a Position-Dependent Motion System, in: Proceedings of the 2017 American Control Conference, Seattle, Washington, 2017, p. [to appear].
[26] D. H. Owens, B. Chu, Modelling of non-minimum phase effects in discrete-time norm optimal iterative learning control, International Journal of Control 83 (10) (2009) 2012–2027.
[27] D. H. Owens, B. Chu, E. Rogers, C. T. Freeman, P. L. Lewin, Influence of Nonminimum Phase Zeros on the Performance of Optimal Continuous-Time Iterative Learning Control, Transactions on Control Systems Technology 22 (3) (2014) 1151–1158.
[28] K. L. Moore, Iterative Learning Control for Deterministic Systems, Springer-Verlag, 1993.
[29] R. Middleton, J. Chen, J. Freudenberg, Tracking sensitivity and achievable H_∞ performance in preview control, Automatica 40 (8) (2004) 1297–1306.
[30] A. Saberi, P. Sannuti, Squaring Down by Static and Dynamic Compensators, Transactions on Automatic Control 33 (4) (1988) 358–365.
[31] B. Kouvaritakis, A. MacFarlane, Geometric approach to analysis and synthesis of system zeros Part 2. Non-square systems, International Journal of Control 23 (2) (1976) 167–181.
[32] A. Stoorvogel, J. Ludlage, Squaring down and the problems of almost zeros for continuous-time systems, Systems & Control Letters 23 (5) (1994) 381–388.
[33] R. van Herpen, T. Oomen, E. Kikken, M. van de Wal, W. Aangenent, M. Steinbuch, Exploiting additional actuators and sensors for nano-positioning robust motion control, Mechatronics 24 (6) (2014) 619–631.
[34] S. Devasia, B. Paden, Stable Inversion for Nonlinear Nonminimum-Phase Time-Varying Systems, Transactions on Automatic Control 43 (2) (1998) 283–288.
[35] A. Pavlov, K. Y. Pettersen, A New Perspective on Stable Inversion of Non-minimum Phase Nonlinear Systems, 7th IFAC Symposium on Nonlinear Control Systems 40 (12) (2007) 527–532.
[36] M. Sato, Inverse system design for LPV systems using parameter-dependent Lyapunov functions, Automatica 44 (4) (2008) 1072–1077.
[37] K.-S. Kim, Q. Zou, Model-less Inversion-based Iterative Control for Output Tracking: Piezo Actuator Example, in: Proceedings of the 2008 American Control Conference, Seattle, Washington, 2008, pp. 2710–2715.
[38] R. de Rozario, A. J. Fleming, T. Oomen, Iterative Control for Periodic Tasks with Robustness Considerations, Applied to a Nanopositioning Stage, in: Proceedings of the 7th IFAC Symposium on Mechatronic Systems, Loughborough, UK, 2016, pp. 623–628.
[39] J. Bolder, S. Kleinendorst, T. Oomen, Data-driven multivariable ILC: enhanced performance by eliminating L and Q filters [to appear], International Journal of Robust and Nonlinear Control.

Appendix A. Background approximate inverse techniques

In this appendix the approximate inverse techniques NPZ-Ignore, ZPETC, and ZMETC are derived for the decomposition in (2). The results are summarized in Table 2.

NPZ-Ignore ignores the nonminimum-phase dynamics by using

$$F(z) = \frac{A(z)}{\beta B_s(z)} \tag{A.1}$$

resulting in

$$H(z)F(z) = \frac{B_u(z)}{\beta}.$$

Parameter β is a tuning parameter and typically used to compensate for the DC gain by setting

$$\beta = B_u(1). \tag{A.2}$$

Note that (A.1) has $p+d$ samples preview. Recalling that ideally $H(z)F(z) = 1$, it follows that for $p > 0$ there is an error in both magnitude and phase.

Zero-phase-error tracking control (ZPETC) perfectly compensates for the phase using

$$F(z) = \frac{A(z)B_u(z^{-1})}{\beta^2 B_s(z)} = \frac{z^{-p}A(z)B_u^*(z)}{\beta^2 B_s(z)}, \tag{A.3}$$

with

$$B_u^*(z) = z^p B_u(z^{-1}).$$

For this choice it follows that

$$H(z)F(z) = \frac{B_u(z)B_u(z^{-1})}{\beta^2} = \frac{z^{-p}B_u(z)B_u^*(z)}{\beta^2}$$

has zero phase as desired. Note that with β in (A.2) the DC gain is compensated and that (A.3) has $p+d$ samples preview.

Zero-magnitude-error tracking control (ZMETC) perfectly compensates the magnitude by using

$$F(z) = \frac{A(z)}{z^p B_s(z)B_u(z^{-1})} = \frac{A(z)}{B_s(z)B_u^*(z)}, \tag{A.4}$$

resulting in

$$H(z)F(z) = \frac{B_u(z)}{z^p B_u(z^{-1})} = \frac{B_u(z)}{B_u^*(z)}. \tag{A.5}$$

Note that (A.5) indeed has zero magnitude error (i.e., unity magnitude) and that (A.4) has d preview samples.